Supplementary Information

Controlling the rheo-electric properties of graphite/carbon black suspensions by 'flow switching'

Thomas Larsen[1,2,*], John R. Royer[3], Fraser H. J. Laidlaw[3], Wilson C. K. Poon[3], Tom Larsen[2], Søren J. Andreasen[2], and Jesper de C. Christiansen[1]

[1] *Department of Materials and Production, Aalborg University, Denmark*

[2] *Advent Technologies A/S, Denmark*

[3] *School of Physics and Astronomy, The University of Edinburgh, Scotland*

[*] *Corresponding author: Thomas Larsen, larsenn.thomas@gmail.com*

Dielectric spectra

Dielectric spectroscopy was employed to analyze the low-frequency (dc) conductivity, σ_{dc}, of the suspensions after different shear histories. From the spectra in Figure S1 we observe a peak in the loss permittivity, ϵ_{r}'', at frequencies of $\sim 10^3 - 10^5$ Hz, depending on the shear history. Additionally, a conductivity contribution to ϵ_{r}'' of the samples is seen at low frequencies. Due to the slope of -1 possessed by ϵ_{r}'' in this region, we surmise its origin to be electronic [1] and fit the expression $\epsilon_{\mathrm{r}}'' = \sigma_{\mathrm{dc}}/\left(2\pi f \epsilon_0\right)$ to the data within the shaded grey region, allowing us to estimate the dc conductivity.

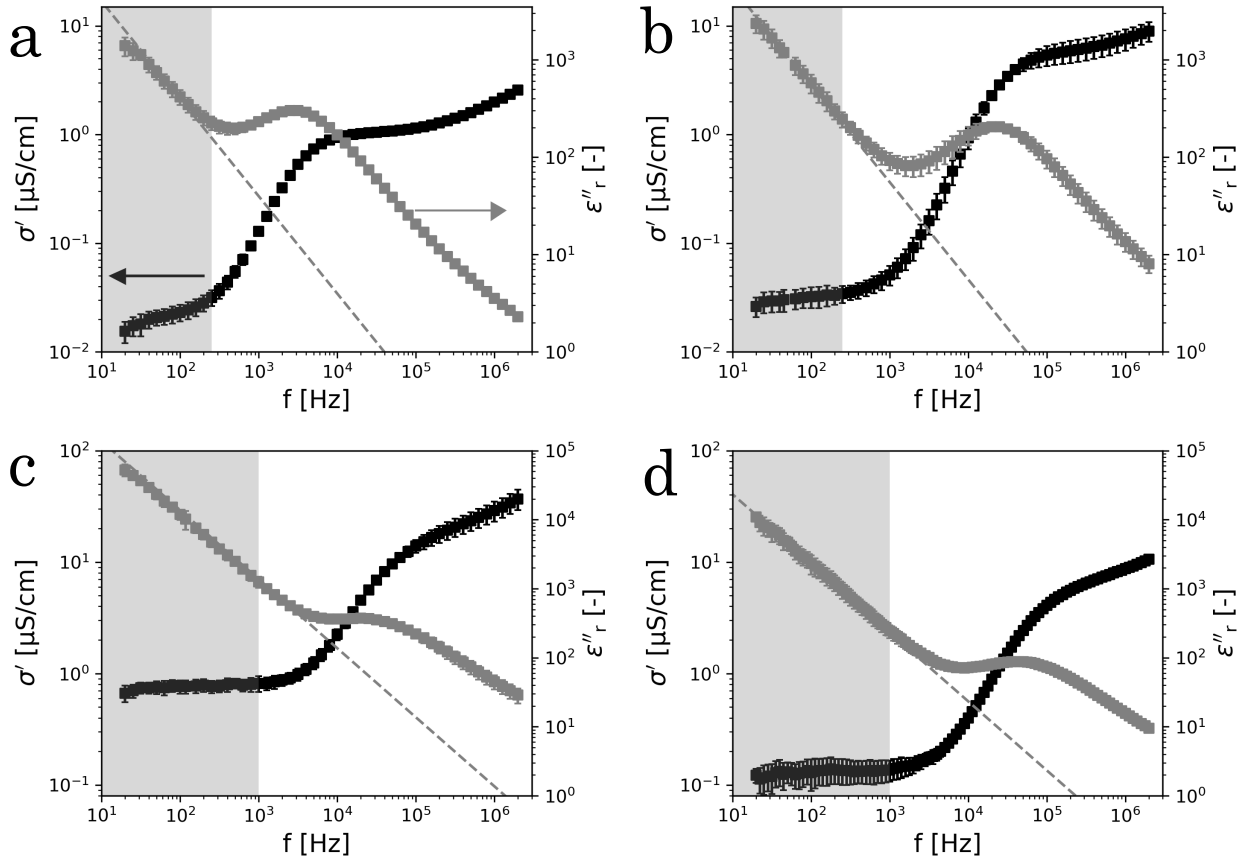

Figure S1: Dielectric spectra (obtained at 100 mV) of quenched and ramped-down (RD, 300 s/step) 6 wt.% carbon black (CB6) and 6 wt.% carbon black + 24 wt.% graphite (CB6/G24) in heavy mineral oil 1000 s after the end of the deformation protocols. (a) CB6 quenched. (b) CB6 RD. (c) CB6/G24 quenched. (d) CB6/G24 RD. The dashed lines are fits of ϵ_{r}'', within the shaded grey region, to the expression $\epsilon_{\mathrm{r}}'' = \sigma_{\mathrm{dc}}/\left(2\pi f \epsilon_0\right)$, and thus they indicate a slope of -1. Error bars show ± 1 standard deviation resulting from at least two measurements.

Transient shear stress data

The transient data used to obtain the flow curves in Figure 1a is shown in Figure S2a-d. After stepping down to a lower shear rate ($\dot{\gamma} \leq 1$ s^{-1} and $\dot{\gamma} \leq 10$ s^{-1} for the gel and composite, respectively), both the gel and composite exhibit a recovery-then-decay of the shear stress, similar to previous reports on oil-based carbon black gels [2]. This response appears more pronounced in the step-down protocol compared to the ramp-down protocol.

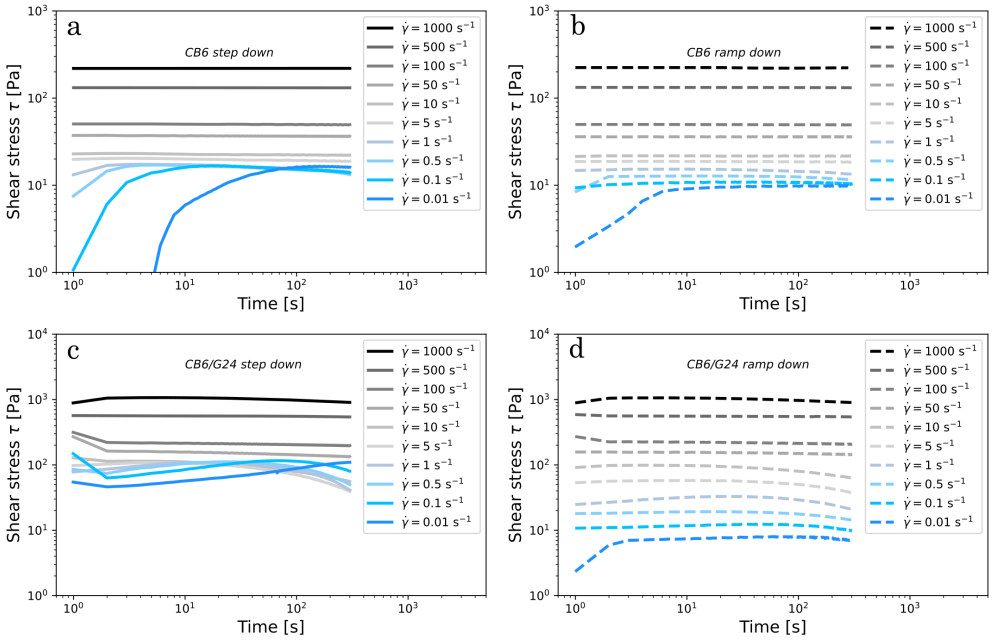

Figure S2: Transient shear stress data used to obtain the data in Figure 1a in the main article. (a) 6 wt.% carbon black, step-down protocol. (b) 6 wt.% carbon black, ramp-down protocol. (c) 6 wt.% carbon black + 24 wt.% graphite, step-down protocol. We verified that no significant increase in τ occured after 300 s at $\dot{\gamma} = 0.01$ s^{-1}, and that stress decay was observed at later times. (d) 6 wt.% carbon black + 24 wt.% graphite, ramp-down protocol.

Influence of graphite content on flow curves and conductivity

To check the generality of our results and examine the influence of graphite on the composite properties, we vary the graphite mass fraction in the composites. The resulting flow curves (Figure S3a) exhibit strong history dependence at all graphite concentrations, unlike the pure graphite suspension (Figure S3a inset). Moreover, adding graphite to the gel monotonically enhances the yield stress and conductivity (Figure S3b) of high-shear rejuvenated composites; the large graphite grains serve as junctions that transfer stresses [3] and contribute to bulk conductivity. Furthermore, the dc conductivities of the quenched composites remain above those measured in the ramped-down composites.

The differences in the flow curves and conductivities after the two protocols diminish as the graphite content is lowered. We do not yet fully understand this effect in our composites, but it was shown for the silica-based binary system in [4] that upon lowering the fraction of large fillers the bistable behavior was eventually lost. Nevertheless, our results show that a homogeneous dispersion of carbon black and graphite fillers, relative to a heterogeneous microstructure, is beneficial to both strength and conductivity in these composites.

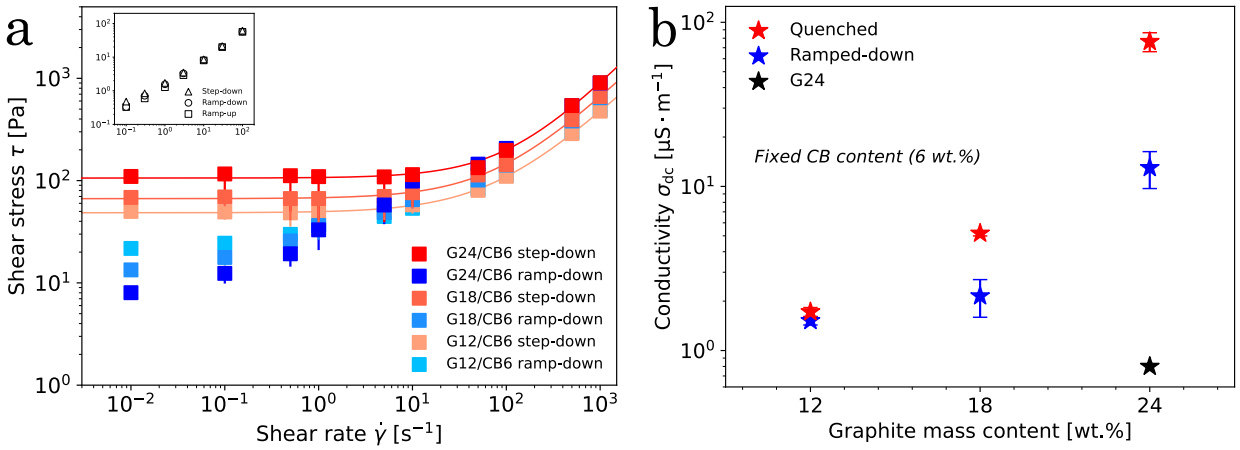

Figure S3: (a) Flow curves of composites with 12, 18 and 24 wt.% graphite mixed with 6 wt.% carbon black in heavy mineral oil. Each data point is measured for 300 s, so the vertical line show the stress decay after the stress maximum. The solid lines are Herschel-Bulkley model fits to the step-down curves and clearly show the increase in yield stress with graphite content. Inset: flow curves of 24 wt % graphite in mineral oil obtained by (i) stepping down from $\dot{\gamma} = 100$ s^{-1} to a lower shear rate for 60 s which was sufficient for reaching a steady state, (ii) ramping down at 300 s/step and (iii) subsequently ramping up at the same rate. Clearly, the graphite suspension rheology is protocol-independent. (b) Low frequency (dc) conductivity as a function of graphite mass content for composites either (i) quenched from $\dot{\gamma} = 1000$ s^{-1} to rest, or (ii) after the ramp-down protocol. Quenching from a high shear rate produces composites with highest conductivities. For comparison, we included the conductivity of a 24 wt % graphite in mineral oil suspension. Error bars denote ± one standard deviation based on at least two measurements.

Temporal evolution of carbon black/oil suspension conductivity

When sheared in a confined geometry, carbon black (CB) particles dispersed in a hydrocarbon tend to form vorticity-aligned log-rolling structures [5–7]. Grenard et al. showed that for CB in mineral oil this self-organization occurs at a gap-dependent, but concentration-independent, critical shear rate, $\dot{\gamma}_c$, which for their particular CB (Cabot Vulcan XC72R) was described by $\dot{\gamma}_c = 3650 \cdot h^{-\alpha}$ [6]. Here, h is the gap height in μm and $\alpha = 1.4 \pm 0.1$. As a rough approximation, we assume the same gap-dependence of $\dot{\gamma}_c$ applies to our CB suspension, resulting in $\dot{\gamma}_c = 0.2 - 0.6$ s^{-1} for $h = 800$ μm. Based on these considerations, we shear the 6 wt.% CB suspension (CB6) at three different shear rates $\left(\dot{\gamma} = 1 \text{ s}^{-1},\ 10 \text{ s}^{-1},\ 100 \text{ s}^{-1}\right)$ for a range of accumulated strains and measure the conductivity at rest, Figure S4. Independent of the accumulated strain, the conductivity remains almost constant at ~ 1.4 μS cm^{-1} when shearing at $\dot{\gamma} = 10 - 100$ s^{-1}, suggesting the microstructure remains largely unchanged. A noticeable difference, however, occurs when shearing at $\dot{\gamma} = 1$ s^{-1}; the conductivity goes through a maximum at $\gamma = 200$ after which it decreases to levels observed at $\dot{\gamma} = 10 - 100$ s^{-1}. Such a conductivity increase at low shear rates (stresses) was attributed to the formation of log-rolling flocs in an 8 wt.% CB in light mineral oil [8]. Furthermore, the accumulated strain of $\gamma = 200$ at which the conductivity is largest agrees with the reported accumulated strains necessary for CB, and other particles, to form log-rolling flocs ($\gamma = 200$ by Osuji and Weitz [5], a few hundred strain units by Varga et al. [7]).

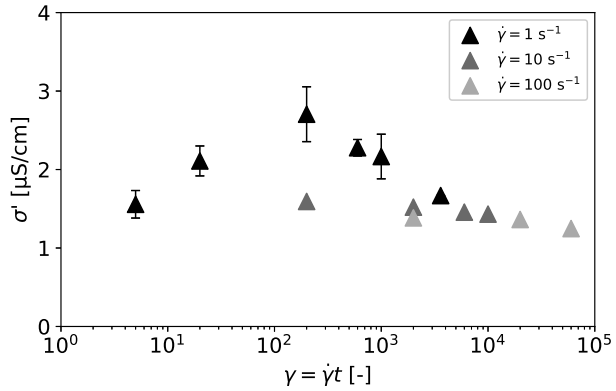

Figure S4: Conductivity, σ', as a function of accumulated strain, $\gamma = \dot{\gamma}t$, for the 6 wt.% carbon black in oil at various constant shear rates, $\dot{\gamma}$. The conductivity was measured at rest just after cessation of shear for the desired amount of time, and the geometry was a 25 mm diameter smooth parallel plate with a gap height of $h = 800$ μm. During conductivity measurements, the AC voltage was 100 mV and the frequency 10^5 Hz. Data of samples with error bars, indicating ± 1 standard deviation, is based on two measurements.

Additionally, we tested this hypothesis by dispersing 2 wt.% CB in heavy mineral oil by bath sonication. Afterwards, ≈ 0.1 wt.% Nile red (Sigma Aldrich) was dissolved in the suspension by roller mixing the resulting mixture for several hours. We then performed imaging with a Leica SP5 confocal microscope *in situ* in an Anton Paar MCR301 rheometer using a 40 mm diameter roughened parallel plate with a gap height of 250 μm. The resulting snapshots in Figure S5, taken at various accumulated strains, show carbon black and mineral oil as the black and green phase, respectively. The microstructure is seen to evolve from a relatively homogeneous state (upper row) to a more or less phase separated state around $\gamma \approx 200$ (middle row) with large log-like CB structures oriented along the vorticity direction. Shearing for longer times results in the flocs being broken up (bottom row), in accordance with reports by Osuji and Weitz [5].

The accumulated strain at which log-rolling flocs are present in the confocal microscopy images agrees with the conductivity maximum, both at $\gamma \approx 200$. The continued shearing, causing destruction of the flocs, is similarly consistent with the decreased conductivity which is likely due to the concomitant increase in separation between aggregates. Although the suspension investigated by rheo-confocal imaging is less dense than the one from which conductivity results are obtained, we argue the comparison is valid since the formation of vorticity-aligned flocs has been visually

observed to occur in a range of CB concentrations in mineral oil [6].

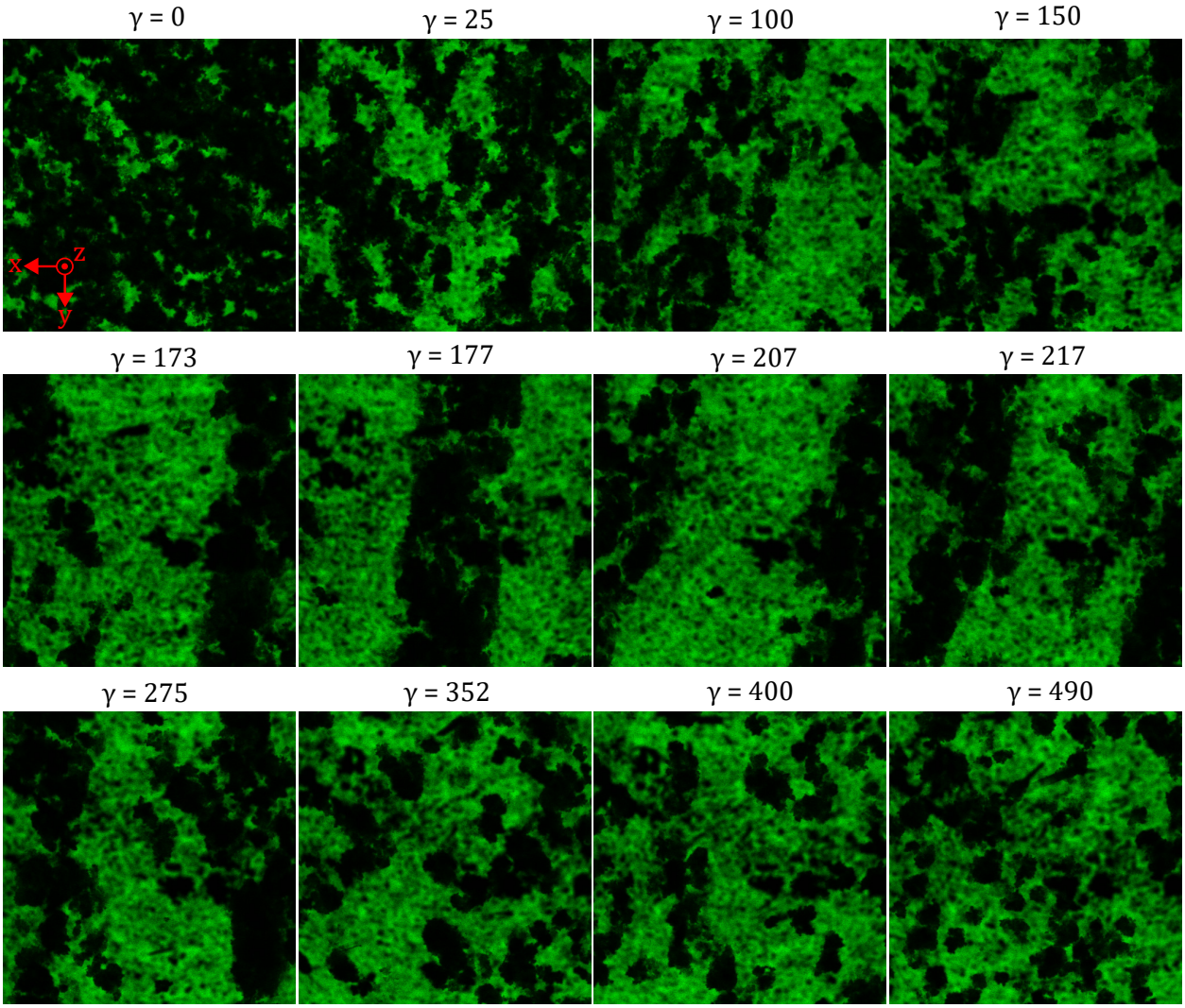

Figure S5: Confocal microscopy images at various accumulated strains, γ, of 2 wt.% carbon black in heavy mineral oil sheared at $\dot{\gamma} = 0.1$ s^{-1}. The images are taken in the flow-vorticity $(x - y)$ plane at a height of $z = 50$ μm. Carbon black appears black while the mineral oil is seen as the green phase. We used a 10× objective, and each frame covers an area of 931.82 μm × 931.82 μm.

Large-area cryo-SEM images

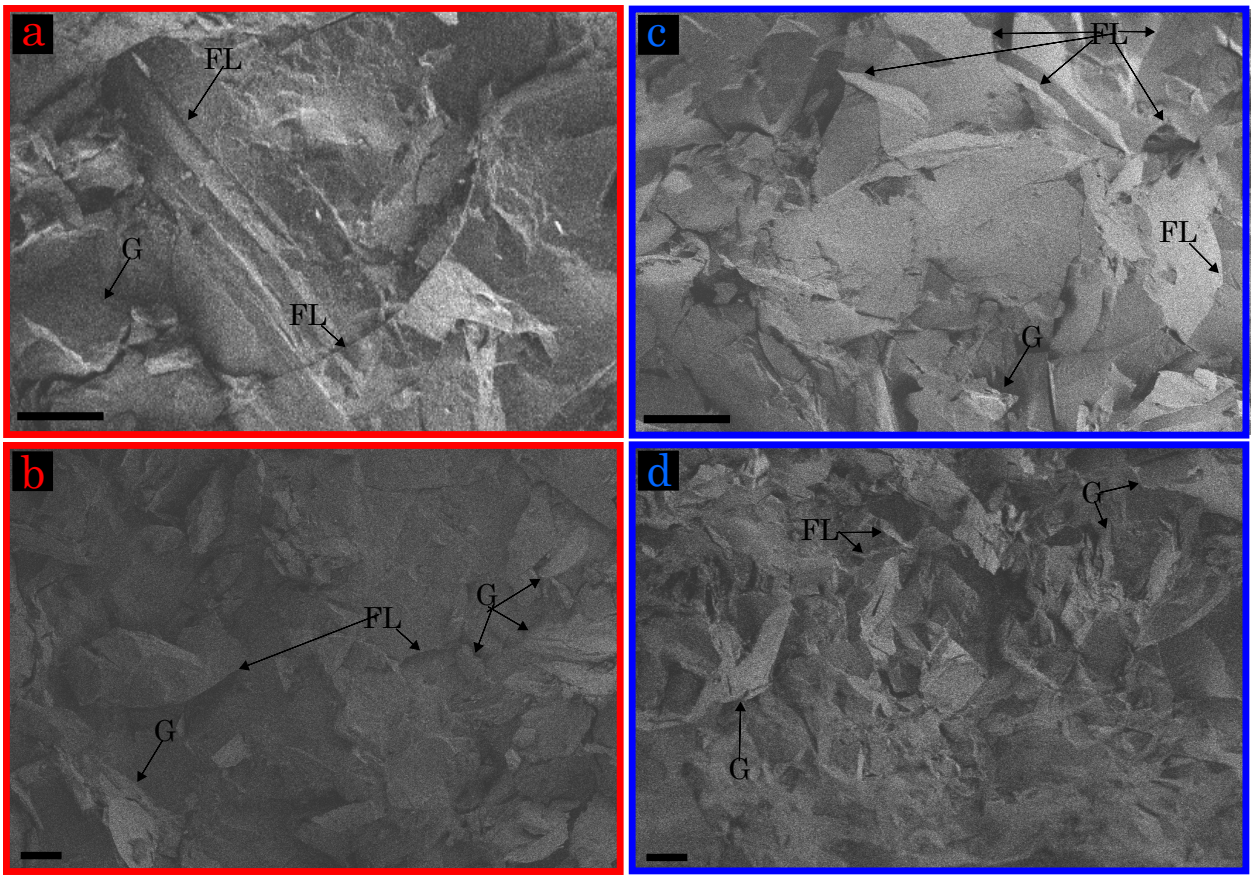

Figure S6: Secondary electron secondary ion (SESI) signal micrographs of the InLens cryo-SEM images in the main article. Specifically, (a,b) correspond to Figures 2a and 3a while (c,d) correspond to Figures 2c and 3b. The rough topography of the surface due to sample preparation is clearly visible in all images. This causes fracture lines (FL) to be clearly visible whereas the graphite (G) particles are hard to identify. Carbon black particles are not discernible in these images. All scale bars indicate 10 μm.

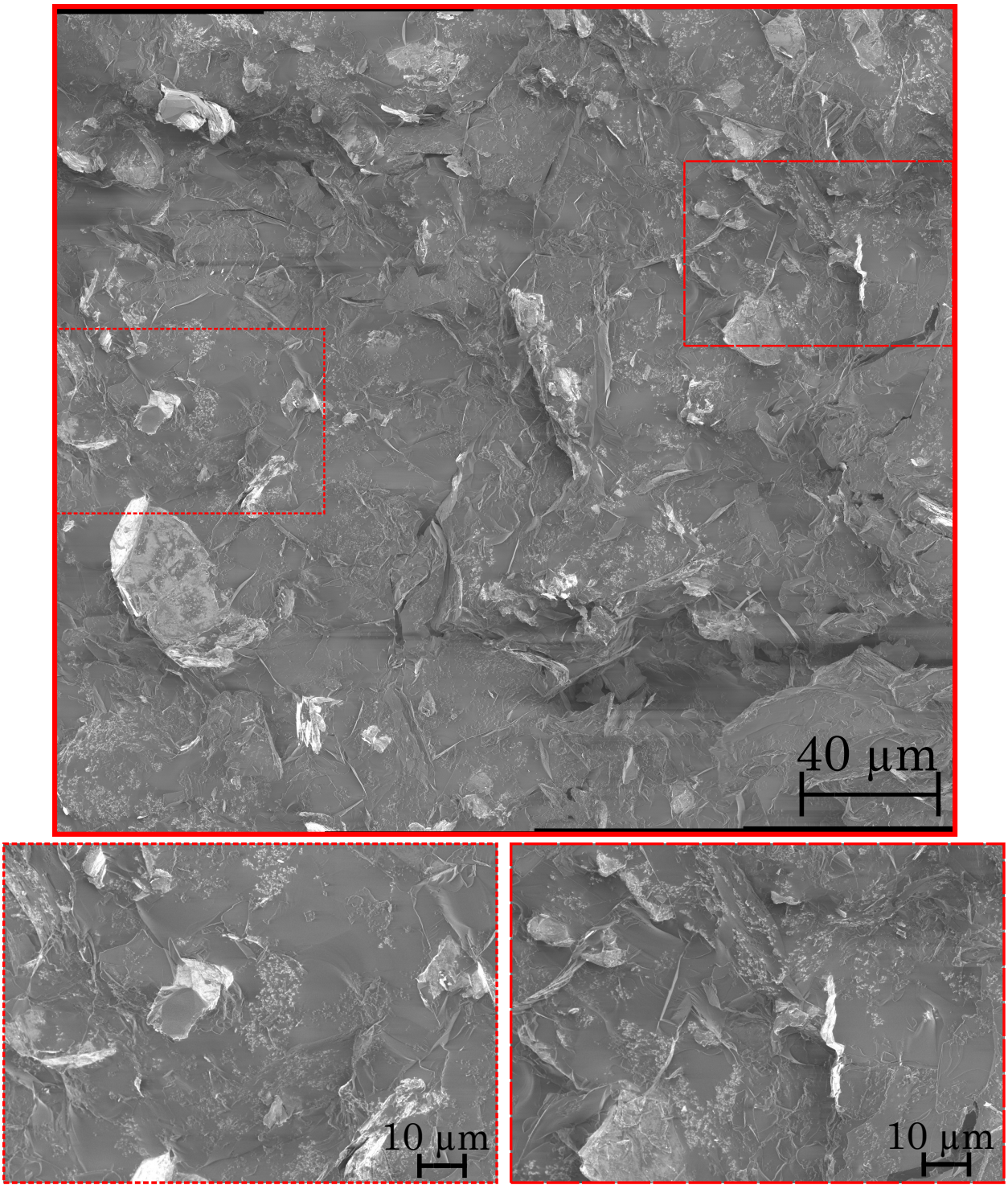

Figure S7: Cryo-SEM image and photo of CB6/G24 after the step-down protocol in steady shear. Magnification was 1500× in the cryo-SEM image, and stitching of the individual images was performed with ImageJ. The area covered by the fused image is 0.060 mm^2. Carbon black is seen as small, bright aggregates while graphite appears as larger, bright flakes.

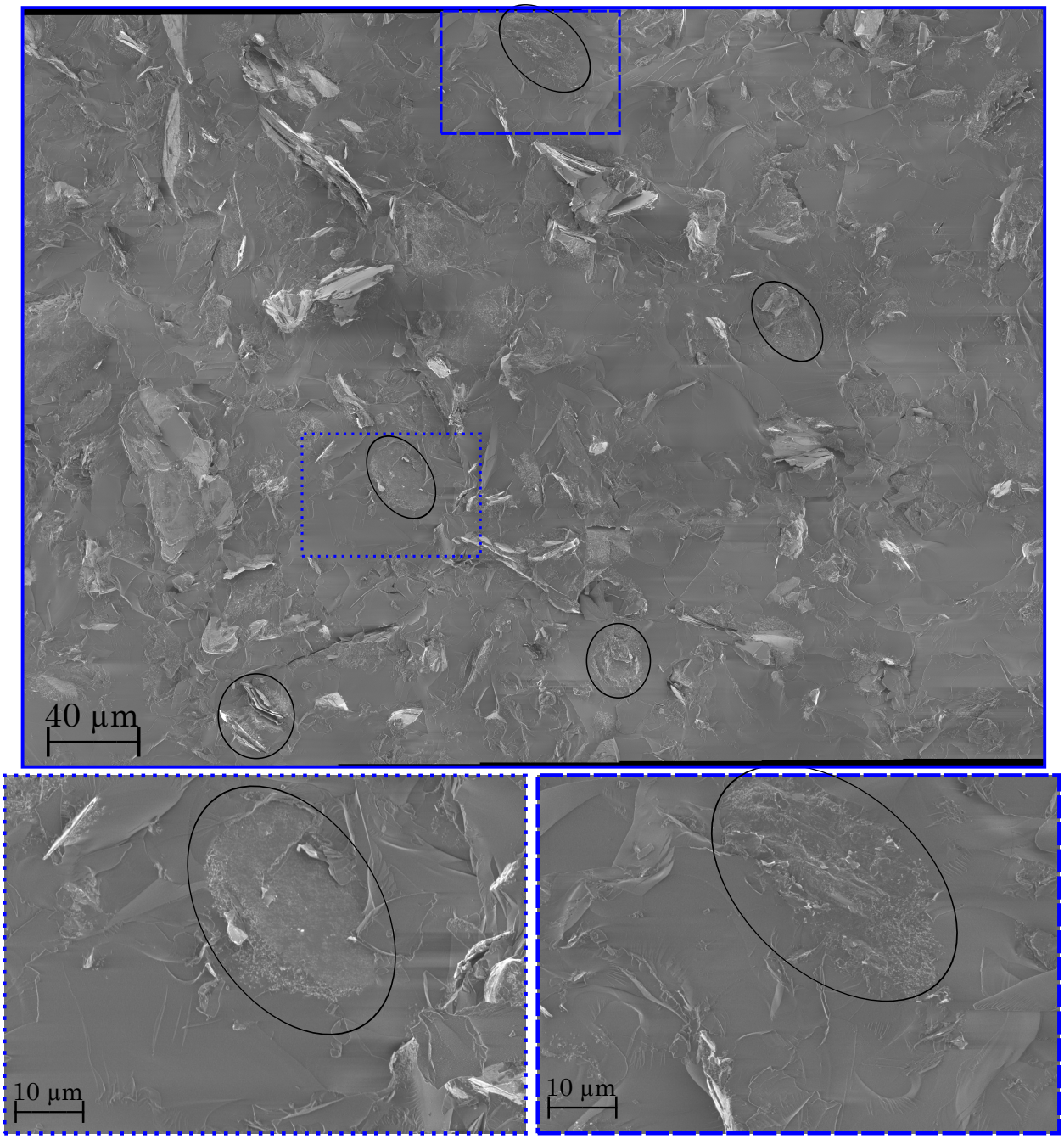

Figure S8: Cryo-SEM image and photo of CB6/G24 after the ramp-down protocol in steady shear. Magnification was 1500× in the cryo-SEM image, and stitching of the individual images was performed with ImageJ. The area covered by the fused image is 0.15 mm^2. Black circles: examples of 'blobs'. Carbon black is seen as small, bright aggregates while graphite appears as larger, bright flakes.

Pure gel cryo-SEM images

Similarly to the composite in Figure 2 and 3 in the main article, we imaged the pure carbon black gel (6 wt.% carbon black in heavy mineral oil) after quenching from a high-shear state ($\dot{\gamma} = 1000$ s^{-1}) and following the ramp-down protocol. Unlike in the composite, the resulting microstructures look similar, Figure S9a and b, which may reflect why the two shear protocols produce relatively similar flow curves (Figure 1a) and conductivities (Figure 1d). Structural characterization techniques would, however, be useful to quantify any differences in, e.g., fractal dimension of clusters [9] and their sizes [10] in the two states.

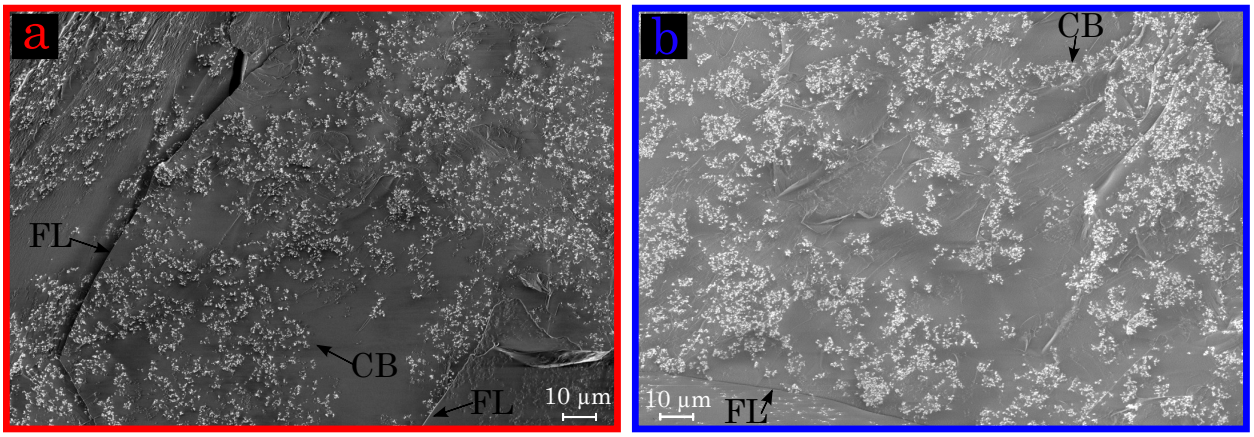

Figure S9: Cryo-SEM image and photo of 6 wt.% carbon black in heavy mineral oil (CB6) after (a) quenching from a high shear state ($\dot{\gamma} = 1000$ s^{-1}) and (b) the ramp-down protocol. Carbon black (CB) is seen as small, bright aggregates. Additionally, fracture lines (FL) are visible on the surface.

Transient creep data

In Figure S10 we show selected transient shear rate-data used to determine the composite (6 wt % carbon black + 24 wt % graphite in oil) yield stress, τ_y, after various preshear and sample preparation histories. The top row (a-c) are data measured on the initially homogeneous composite (*pre*-preshear at $\dot{\gamma} = 1000$ s^{-1} for 300 s), while the bottom row (d-f) are from the initially heterogeneous composite (*pre*-preshear at $\dot{\gamma} = 10$ s^{-1} for 1000 s). The yield stress (dashed horizontal line in the legends) is taken to lie between the largest stress where creeping flow is observed, and the lowest stress where the shear rate approaches a plateau due to steady flow. Yield stresses were determined from the remaining creep test-data (not shown here) in a similar manner.

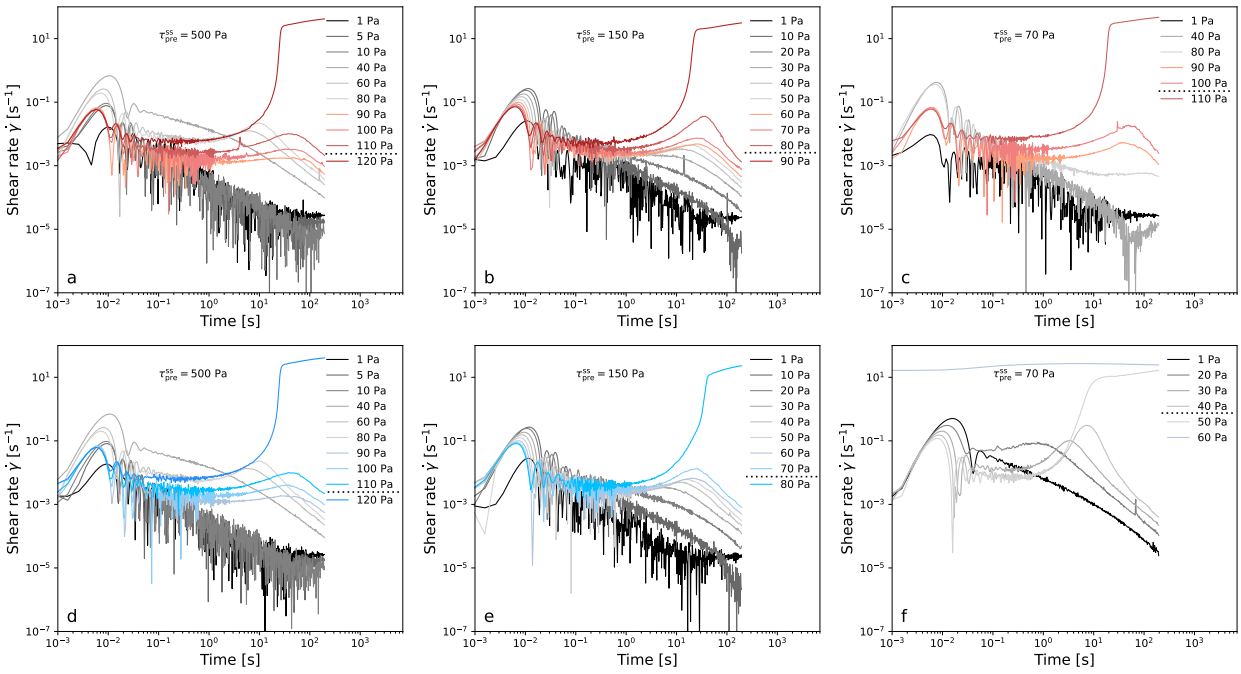

Figure S10: Transient shear rate during creep tests after shearing the composite () at the indicated preshear stresses, τ^{ss}_{pre}. The composites were initially (a-c) in a homogeneous state obtained by preshear at $\dot{\gamma} = 1000$ s^{-1} for 300 s, or (d-f) in a heterogeneous state obtained by preshear at $\dot{\gamma} = 10$ s^{-1} for 1000 s. The dashed line in the legend denotes the location of the yield stress in between a creeping and flowing sample.

References

1. Schönhals, A. & Kremer, F. in *Broadband Dielectric Spectroscopy* (eds Kremer, F. & Schönhals, A.) 59–96 (Springer-Verlag Berlin Heidelberg, 2003).

2. Wang, Y. & Ewoldt, R. H. New insights on carbon black suspension rheology—Anisotropic thixotropy and antithixotropy. *J. Rheol.* **66,** 937–953 (2022).

3. Jiang, Y. *et al. Filled Colloidal Gel Rheology: Strengthening, Softening, and Tuneability* 2023. arXiv: `2311.08751 [cond-mat.soft]`.

4. Jiang, Y., Makino, S., Royer, J. R. & Poon, W. C. K. Flow-Switched Bistability in a Colloidal Gel with Non-Brownian Grains. *Phys. Rev. Lett.* **128,** 248002 (2022).

5. Osuji, C. O. & Weitz, D. A. Highly anisotropic vorticity aligned structures in a shear thickening attractive colloidal system. *Soft Matter* **4,** 1388–1392 (2008).

6. Grenard, V., Taberlet, N. & Manneville, S. Shear-induced structuration of confined carbon black gels: steady-state features of vorticity-aligned flocs. *Soft Matter* **7,** 3920–3928 (2011).

7. Varga, Z. *et al.* Hydrodynamics control shear-induced pattern formation in attractive suspensions. *Proc. Natl. Acad. Sci. U.S.A.* **116,** 12193–12198 (2019).

8. Helal, A., Divoux, T. & McKinley, G. H. Simultaneous Rheoelectric Measurements of Strongly Conductive Complex Fluids. *Phys. Rev. Appl.* **6,** 064004 (2016).

9. Dagès, N. *et al.* Interpenetration of fractal clusters drives elasticity in colloidal gels formed upon flow cessation. *Soft Matter* **18,** 6645–6659 (2022).

10. Hipp, J. B., Richards, J. J. & Wagner, N. J. Structure-property relationships of sheared carbon black suspensions determined by simultaneous rheological and neutron scattering measurements. *J. Rheol.* **63,** 423–436 (2019).